A FRAMEWORK FOR THE TRANSMISSION OF MULTIMEDIA TRAFFIC USING HM AND RS CODING OVER NAKAGAMI-M CHANNELS

T. Quazi*, H. Xu and A. Saeed*****

School of Engineering, Electrical, Electronic and Computer Engineering Building, Howard College Campus, University of KwaZulu-Natal, Durban, 4041, South Africa.
**E-mail: quazit@ukzn.ac.za **E-mail: xuh@ukzn.ac.za ***E-mail: asaeed09@gmail.com*

Abstract: Hierarchical modulation (HM) provides different levels of error performance for the high and low priority bits modulated. This differentiation can be aligned to various classes of multimedia traffic demanding different levels of error rate performance. In a previous cross-layer design scheme, which combined conventional modulation at physical layer with RS coding at the application layer, an unequal error protection mechanism was used at the application layer for guaranteeing quality of service for various classes of multimedia traffic. Instead of using only a single layer, in this paper we present a more flexible two layer cross-layer design framework for unequal error protection, combining RS coding at the application layer with HM at the physical layer. Furthermore, in order to improve error performance of the system, a signal space diversity (SSD) scheme is also incorporated into the physical layer of the framework. Without consuming additional transmit power and bandwidth, the use of the SSD HM in the cross-layer design system resulted in significant gains when compared to the non-SSD, standard HM system. It is shown that the cross-layer design system with SSD HM has a 10dB gain over the non-SSD HM system in a Nakagami m=1 channel with a frame error rate target of 10^{-4}.

Keywords: Cross-layer design, hierarchical modulation, multimedia traffic, unequal error protection, signal space diversity.

1. INTRODUCTION

One of the fundamental requirements of future-generation mobile networks is the support for multimedia traffic such as voice, video and data. Previously these classes of traffic would be transmitted separately but as demand for efficiency increases, so does the need to transmit these various classes of traffic simultaneously in mixed traffic transmission frames [1]. One of the methods considered recently for the simultaneous transmission of various classes of traffic with differentiated levels of quality of service is hierarchical modulation [2]. In HM, a single physical layer bit stream can be separated into several multiplexed sub-streams with different levels of priority and receive different or unequal error protection (UEP), which conventional modulation schemes cannot achieve.

Forward error correction (FEC) codes, such as rate compatible punctured convolutional codes (RCPC), turbo codes, low-density parity check (LDPC) codes, have been used for providing UEP to bits of unequal importance in methodologies labelled as joint source channel coding (JSCC). This has primarily been in the application area of image or video transmission [3]. However, unlike such coding schemes HM can support UEP without adding (varying) redundancy to the transmitted data. As an example, if two classes of multimedia traffic are being transmitted using HM: data and voice, the data stream (with a lower error rate requirement) can be inserted to the high priority (HP) sub-stream of the hierarchical modulation scheme while the voice stream (with a higher error rate requirement) can be multiplexed onto the low priority (LP) sub-stream. HM can also be used to enhance audio/video broadcasting services using its ability to transmit multiple data streams. The HP sub-stream can be used for the base layer of the media transmission while the LP sub-stream can be used for the enhancement layer. All terminals, whether in good or bad channel conditions can receive the base layer, as the only the HP sub-stream can be decoded. However those terminals in good channel conditions can receive both the base and the enhancement layers, as they will be able to decode both the HP and LP sub-streams. This flexible transmission system can be used in media broadcasting systems which allow different resolutions of video display or terminals with variable screen sizes.

The cross-layer design (CLD) methodology has been widely used for the transmission of multimedia traffic over the challenging wireless environment. In previous work [4] studied a CLD used an FEC at the application layer to allow for the transmission of mixed classes of traffic in a single physical layer frame. The scheme in [4] used an adaptive modulation scheme to ensure a baseline bit error rate (BER) performance at the physical layer, while the unequal error protection for the three classes of traffic, namely voice, video and data was provided by a Reed-Solomon (RS) coding mechanism at the application layer. Although functional, this scheme, like many proposed UEP enabling schemes, provided UEP using a single layer, namely the application layer. In this paper, we propose a more flexible two layered unequal error protection framework in which the RS coding UEP mechanism at the application layer is supplemented with

a second UEP mechanism at the physical layer where the efficient UEP capabilities of HM is applied. The reason for the use RS coding in the CLD mechanism over other FEC coding schemes such as LDPC codes is that it is more suited for use in the applications layer as compared to LDPC codes which is more practically applied in the physical layer. The LDPC decoder requires the use of soft information regarding the channel and it is better placed to retrieve this at the physical layer. In addition, LDPC codes, unlike RS codes, are not maximum distance separable (MDS) codes and require a long code length to be effective. RCPC is another FEC scheme that could be considered, but it also requires channel information in order to achieve good performance. RS coding does not have this requirement and is thus used for the proposed UEP CLD scheme.

Without consuming any additional bandwidth, transmit power or space, signal space diversity is a technique which takes advantage of the intrinsic diversity of multi-dimensional constellations to improve BER performance [5]. Thus the system error performance of the proposed CLD scheme is further enhanced by the incorporation of SSD into the physical layer. It will be shown that this significantly improves the error rate performance at the physical layer and consequently the performance of the overall CLD scheme.

2. Related Work

The CLD schemes for the handling of multimedia traffic have traditionally focused on the transmission of scalable video or progressive image data over varying channel wireless links [3]. The concept is to encode the source video/image data such that there is a decreasing level of importance and then to provide UEP depending on the unequal importance. Various types of coding schemes have been used for the purposes of designing joint source channel coding video/image multimedia traffic transmission [3]. There have been some schemes proposed that use modulation assisted JSCC such as the one in [6] which uses a three level LDPC code and a quadrature phase-shift keying (QPSK)/16 quadrature amplitude modulation (16QAM) combination for providing UEP. The limitation of using coding schemes for providing the wide range of UEP required for multimedia traffic is that, consequently, a wide range of redundant data has to be added to the transmitted data. This limitation can be overcome by the use of hierarchical modulation which can achieve UEP without adding redundancy [1].

HM is a popular strategy for providing UEP and has been included in various standards such as Digital Video Broadcast-Terrestrial (DVB-T). HM has been combined with channel coding for UEP in the transmission of progressive image in [3] and data partitioned video in [7]. HM has also been included in the DVB-H standard, and [8] presents a study of HM combined with scalable video coding (SVC) for Mobile TV. These schemes restrict the definition of multimedia traffic to video and image data. Although the multimedia traffic is more generalized in [1] and [2] which use HM for UEP, these schemes only focus on the physical layer, while the CLD framework studied in this work looks at combining two layers where an application layer FEC scheme is combined with HM at the physical layer for providing UEP for various classes of multimedia traffic. Furthermore in a recent study, [9] has shown that incorporating an SSD mechanism to HM significantly improves the system BER performance in a fading channel. Thus the same SSD is combined with HM at the physical layer of the CLD scheme to improve its overall error rate performance.

A study of a LDPC coded HM system has been presented in [10-11]. There is a strong coupling between the HM modulator/demodulator and the LCPC encoder/decoder of the scheme in the studies, and since the LDPC decoder requires soft information from the channel, the entire system is practically implemented in the physical layer where such information is readily available. An application and physical layer cross-layer UEP scheme is presented in [12]. The FEC code used at the application layer is based on RS codes, and HM is used at the physical layer, however the system restricts the traffic to video data only while in this work multimedia traffic is considered more generally. The system proposed in this paper also incorporates the SSD HM mechanism to the physical layer for improved error rate performance. SSD is considered an important enhancement technology for the next generation DVB standard, namely DVB-T2 [13]. Constellation rotation has been combined with HM in [14-15], however in both these systems, the objective is to increase the error performance of the LP sub-stream transmission, whereas, the SSD HM scheme in this paper considers both sub-streams. In summary, none of the schemes listed here considers a system that combines an application layer FEC scheme with SSD enhanced HM scheme as it is done in the proposed system.

The remainder of the paper is organized as follows. Section 3 describes the system model and the two configurations of the proposed CLD framework. In the first configuration the application layer FEC coding scheme is combined with a typical HM scheme while in the second it is combined with a SSD HM scheme. Section 4 presents the theoretical system performance which is then verified using simulation results. Section 5 concludes the paper.

3. System Model

The architecture for the two layer UEP CLD mechanism is shown in Figure 1.

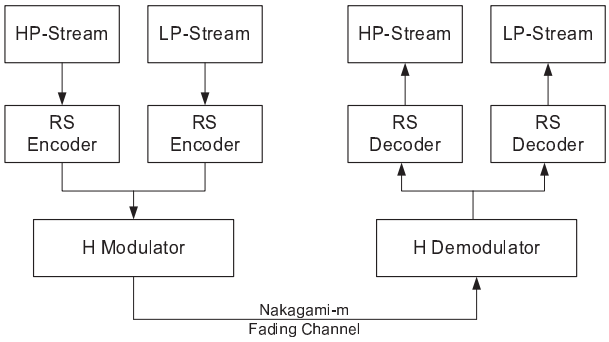

Figure 1 HM and RS CLD system model.

The multimedia traffic is generated by different applications and each stream will have its own error performance requirement. The structure in Figure 1 shows a high and low priority stream (labeled HP and LP respectively), but this could be generalized to accept more streams and the system would then be appropriately scaled. Each stream is then sent to the application layer FEC module where each stream is encoded by an RS encoder to produced RS code blocks/frames. The frames are sent next to the physical layer where the proposed system has two possible configurations. In the first configuration, the data from the RS encoder is modulated using the standard hierarchical quadrature amplitude modulation (HQAM), while in the second a SSD HQAM mechanism is used. The modulated signal is then transmitted over a Nakagami-*m* fading channel.

At the receiver, the (generalized) received signal is given by $r = hu + n$ where u is the transmitted signal, n the additive white Gaussian noise which is modeled as a zero-mean complex Gaussian random variable with variance $N_0/2$ per dimension, where N_0 is the single-sided power spectrum density of the noise; and h is the fading coefficient. The amplitude of the fading is modeled as the Nakagami-*m* distributed random variable according to

$$f(\beta) = \frac{2}{\Gamma(m)}\left(\frac{m}{\Omega}\right)^{m} \beta^{2m-1} exp\left(-\frac{m}{\Omega}\beta^{2}\right) \qquad (1)$$

where m is the Nakagami fading parameter and $\Gamma(m)$ is the Gamma function defined by $\Gamma(m) = \int_0^\infty y^{m-1} exp(-y)dy$ and $\Omega = E[|h|^2]$ is the average fading power, E being the expectation. The received signal is demodulated at the physical layer which leads to the extraction of the HP and LP symbol streams which are then passed to the respective RS decoders for the decoding of the particular traffic data frames. In the next two subsections the two physical layer mechanisms used in the proposed CLD scheme, namely HM and the HM with SSD, are overviewed.

3.1 Hierarchical Modulation

The system in HQAM assumes two separate input bit streams carrying information of unequal importance. In each HQAM symbol, 2 HP bits and $log_2(M) - 2$ LP bits (M is the QAM modulation order) are arranged as follows. The HP bits are assigned to the most significant bit position in the in-phase and quadrature phase of the symbol. The remaining bits positions in the in-phase are assigned $\frac{1}{2}log_2(M) - 1$ LP bits while the other half of the LP bits are assigned to the quadrature-phase. Figure 2 shows Gray encoded HQAM constellation using a 4/16-HQAM system. The HP sub-stream will be transmitted using the 2 MSBs while the LP sub-stream will be transmitted with the 2 low significant bits (LSBs). The level of relative unequal protection between the two streams is controlled by varying two distance parameters: the distance between two symbols in adjacent quadrants and the distance between two neighbouring symbols in the same quadrant ($2a$ and $2b$ in Figure 2 respectively). The ratio $\alpha = \frac{a}{b}$ determines the hierarchy of bit priority and thus the level of UEP, and is commonly referred to as the constellation or hierarchical parameter.

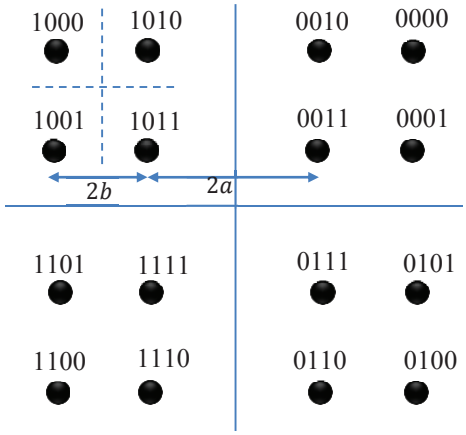

Figure 2 4/16-QAM Hierarchical constellations.

The demodulation process is done by treating each quadrature of the received 4/16-HQAM as a PAM signal and using the decision boundaries as shown in Figure 2, with the solid line for the HP bits and the dashed line for the LP bits [16].

3.2 SSD using Rotated HQAM

In a recent work, [9] has studied the performance of HM with signal space diversity (SSD) for single and multiple antenna configurations. SSD exploits the intrinsic diversity of multidimensional constellation such as HQAM to further improve their error rate performance, and this is done without the cost of additional bandwidth, power or antennas. The only cost of the performance improvement is the increase in complexity at the receiver where maximum-likelihood (ML) detection is required. The procedure for the SSD scheme is shown in Figure 3.

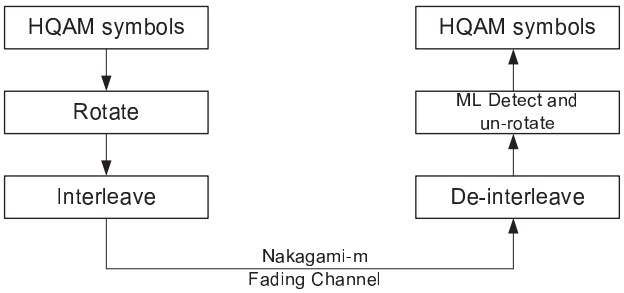

Figure 3 SSD Procedure.

This procedure follows that which is shown in Figure 1. The HQAM symbols $x_i = [x_i^I \quad x_i^Q]$, which have the RS encoded bits, are first rotated to produce a rotated version of the input symbol stream: $\tilde{x_i} = x_i R^\theta$. x_i^I and x_i^Q represent the in-phase and quadrature-components of the HQAM signal and R^θ is given by [9]

$$R^\theta = \begin{bmatrix} \cos\theta & \sin\theta \\ -\sin\theta & \cos\theta \end{bmatrix} \tag{2}$$

The optimum rotation angle θ_{opt} was derived in [9] by maximizing the minimum distance between the unique components of the rotated constellation points. The final expression of the optimization, as shown in (3), is a function of the distance parameters a and b via the hierarchical parameter α.

$$\tan\theta_{opt} = \frac{\alpha}{\alpha + 3} \tag{3}$$

The rotated symbol stream is then arbitrarily grouped into pairs and passed through a component interleaver where the in-phase and the quadrature-phase components in each pair are interleaved to produce new symbol pairs $u_1$and u_2 as shown in (4).

$$\begin{aligned} u_1 &= \tilde{x}_1^I + j\tilde{x}_2^Q \\ u_2 &= \tilde{x}_2^I + j\tilde{x}_1^Q \end{aligned} \tag{4}$$

The symbols $u_1$and u_2 are transmitted on two separate time slots ensuring that each is sent over an orthogonal channel where the transmission is affected by fading and is perturbed by noise. The corresponding signal at the receiver is given by

$$r_i = h_i u_i + n_i \quad i \in \{1,2\} \tag{5}$$

where $i \in \{1,2\}$ is the orthogonal channel time slot index, and h_i and n_i are the fading coefficient and the noise parameter respectively for the corresponding channel index. De-interleaving is performed on a symbol pair to reassemble the in-phase and quadrature-phase components of the original symbols. The symbols are then passed to the ML detector where the availability of full channel state information (CSI) is assumed. The detected signal is thereafter un-rotated using the transpose of the rotation matrix (2) to produce un-rotated HQAM symbols.

4. Performance Analysis

The block diagram of the proposed system in Figure 1 shows that the beginning and end process of the CLD system at the transmitter and receiver is the RS encoder and decoder respectively, thus the system performance is quantified as a function of the HP and LP stream frame error rates (FER) and the first system parameter that affects this is the level protection by the RS encoder at the application layer. The level of error protection provided is determined by number of parity symbols inserted in the RS code frame. The frame error rate (FER) at the receiver is given by

$$P_f = \sum_{k=t+1}^{N} \binom{N}{k} (1 - P_s)^{N-k} P_s^k \tag{6}$$

where each RS code frame has k message symbols to which are appended $N - k$ parity symbols. The correcting potential is determined by the parameter t ($t = F\left[\frac{N-k}{2}\right]$, $F[\cdot]$ is the floor function). Since each RS decoder at the receiver only produces one type/stream of bits i.e. either HP or LP bits, the RS symbol error calculation is only dependent on the BER of one of the streams of data. Thus the symbol error rate (P_s) is given by

$$P_s = 1 - (1 - P_b)^L \tag{7}$$

where P_s represents the symbol error rate for either a HP symbol or LP symbol as shown in Figure 1, P_b the bit error rate of the corresponding HP or LP bits and L the number of bits in the RS symbol. The bits in the RS symbol are assumed to be independent. The physical layer BER achieved is the second parameter that affects the system FER performance and derivations of the two configurations of the proposed system is presented in the following two subsections. Note that FEC is implemented only at the application layer and there is no error correcting coding at the physical layer.

4.1 HQAM BER

The BER of the HP and LP bits of a 4/16-QAM has been analysed in [16]. The BER of HP bits is given by

$$P_{HP}(M) = \frac{1}{2}[P_b(i_1, M) + P_b(q_1, M)] = P_b(i_1, M) \tag{8}$$

where $P_b(i_k, M)$ and $P_b(q_k, M)$ give the BER of the kth in-phase and quadrature phase bits of a 4/16-QAM constellation respectively. The BER of the LP bits is derived by averaging over all the remaining in-phase and quadrate bit as shown in (9).

$$P_{LP}(M) = \frac{2\sum_{k=2}^{\left(\frac{1}{2}\right)\log_2 M} P_b(i_k, M)}{(\log_2 M - 2)} \tag{9}$$

The general BER expressions, $P_b(i_k, M)$, for square 4/M-QAM constellations were derived in [9] and are reported in the Appendix for convenience.

The above method from [16] for determining the BER of HP and LP bits in HQAM used the probability that a transmitted symbol's component exceeds a set boundary. This approach, which is an adaptation of the approach used for standard pulse amplitude modulation (PAM) schemes, is easily applied for standard HQAM where the

components for the symbols have regular distances from the boundaries. However when HQAM with SSD is considered, the HQAM constellations are rotated these distances are no longer regular and thus applying such an approach becomes complicated. In order to derive closed BER expressions for HQAM with SSD, [9] presented accurate approximations for the respective BERs using a simplified nearest neighbourhood (NN) union bound approach. The derivations refer to Figure 4 and for convenience we include the final expressions here.

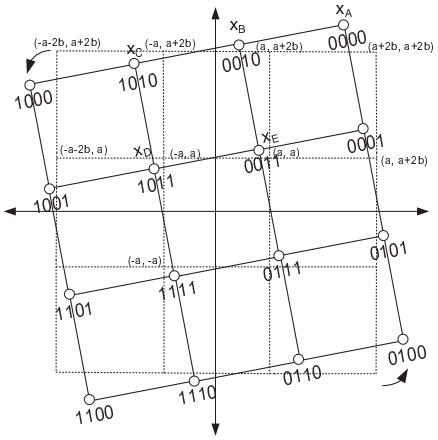

Figure 4 Rotated hierarchical 16-QAM Nearest Neighbour error analysis.

The BER for the HP bits are given by

$$P_{HP} = \frac{1}{2}P(X_B \to X_C) + \frac{1}{4}P(X_B \to X_D) + \frac{1}{4}P(X_E \to X_C). \quad (10)$$

$P(X_B \to X_C)$ represents the pairwise error probability (PEP) of perpendicular neighbhouring symbols of the constellation set and is given by (B1) in the Appendix. $P(X_B \to X_D)$ and $P(X_E \to X_C)$ represent the PEP of diagonal neighbouring symbols is given by (B2) and (B3).

The BER for the LP bits are given by

$$P_{LP} = P(X_A \to X_B), \quad (11)$$

where $P(X_A \to X_B)$ represents the PEP that a transmitted symbol is detected as a perpendicular neighbour within the same quadrant of the received signal and is given by (B4) in the Appendix.

In order to verify the approximate BER expressions derived using the NN approach, we compared the BERs for HP and LP bits using (10) and (11) for standard, un-rotated HQAM with those derived in [16], namely (8) and (9). The Nakagami m parameter used for the comparison is 1 and the hierarchical parameter α used is 2. It can be seen from the curves in Figure 5 that there is a close match between the approximate expressions and those derived in [16]. Thus (10) and (11) are used for determining the theoretical BERs for the HP and LP bits for the standard and the rotated HQAM systems in the following section.

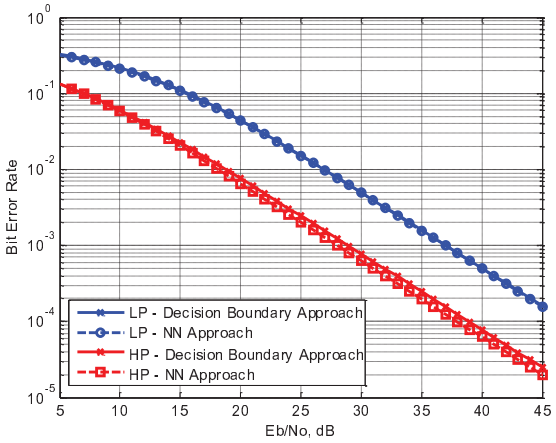

Figure 5 Comparison of two approaches for BER.

5. Simulations and Discussion

The proposed system was implemented in Matlab and was simulated using an accurate Nakagami-m channel model [17]. In this section, the simulation results are compared to the theoretical expressions for the two system configurations, namely RS coding combined with standard HQAM and with rotated HQAM, and it is shown that there is a close match between the two sets of results for both configurations. The parameters varied in the simulation setups are the Nakagami m value, the α value determining the level of hierarchy in HQAM and the t value for varying the level of protection provided by the RS coder.

5.1 RS coded HQAM without SSD

The frame error rate theoretical performance of the two layer UEP CLD system with RS and standard HQAM is shown in Figure 7-8. However, in order to demonstrate the physical layer UEP contribution of the system, the BER performance of the HM layer of the CLD is shown in Figure 6.

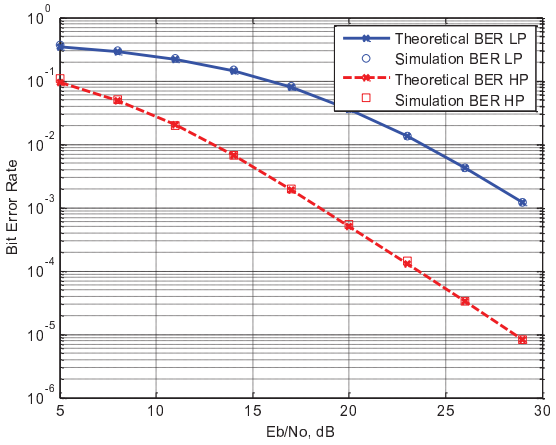

Figure 6 BER of the UEP modulation layer of the CLD with Nakagami-m, m=2, α =3.

In this setup, as well as that for Figure 7, the hierarchical parameter α, which represents the level of UEP between the HP and LP streams is 3. The Nakagami m parameter used for the experiments for Figure 6-8 is 2. As the curves in Figure 6 show, the BER performance for the HP bit stream is much lower than that of the LP bit stream throughout the entire SNR range.

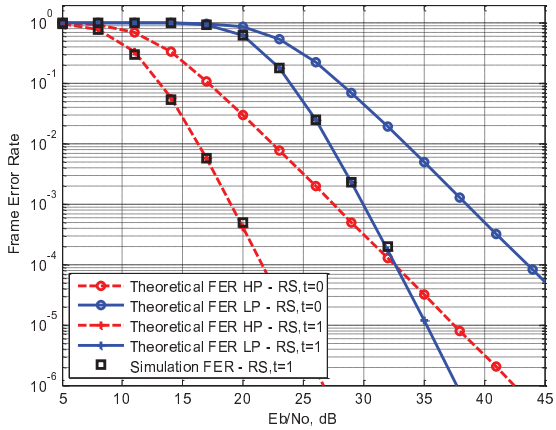

Figure 7 FER of HP and LP streams for two layer UEP CLD in Nakagami-m, m=2, α =3.

The theoretical FER graphs shown in Figures 7 now show the FERs of both the HP and LP streams which are now unequally protected both via the hierarchical modulation as well the RS forward error correcting mechanism. The values N and k for the RS encoder is set to 15 and 13 respectively, and thus the FER curves represent the frame error rate for the system with and without adding 2 parity symbols ($t = 1$) to the RS code block.

In order to highlight the flexibility of the proposed two layer UEP mechanism, the RS and HM parameters are varied while keeping the channel parameter the same and the results are shown in Figure 8. The hierarchical parameter α used in this setup is 2, so this layer provides a lower level of UEP at the physical layer, but the RS parameter t for the HP sub-stream is increased from 1 to 2, thus k is changed from 13 to 11 while N equals 15. This significantly reduces the FER for the HP sub-stream as can be seen from gradient of the 'HP – RS, t = 2' theory and simulation curves which are much steeper as a result of the greater gain relative to the 'LP – RS, t = 1' curves. The combination of the RS coding to the already unequal error protection provided by the HM layer ensures that the HP protected further, thereby increasing the level of unequal error protection achieved. Thus the variable mechanism of the proposed two layer CLD can be used to provide further unequal protection to certain streams of data over others than previous single layered mechanisms.

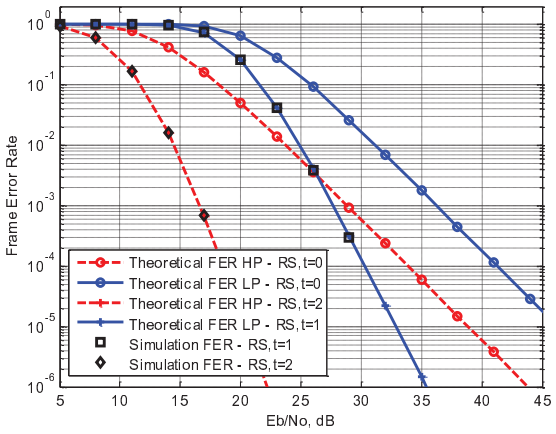

Figure 8 FER of HP and LP streams for two layer UEP CLD in Nakagami-m, m=2, α =2.

5.2 RS coded HQAM with SSD

The effect of incorporating the SSD scheme to the physical layer of the two layer CLD mechanism is presented in this subsection. The graphs in Figure 9 compares the BER of rotated HQAM with the standard HQAM modulation and shows that there are significant gains (approximately 7 dB at BER target of 10^{-3}) as a consequence of adding the SSD scheme. The hierarchical parameter α is set to 3 and the Nakagami m fading parameter is 1.

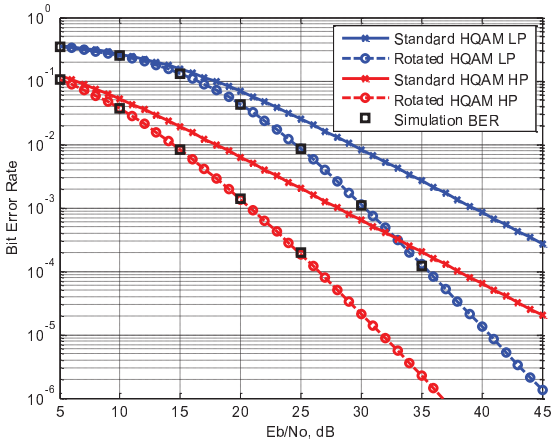

Figure 9 BER of the UEP modulation layer of the CLD with Nakagami-m, m=1, α =3.

The FER performance improvement for the two layer CLD system, with RS coding at the application layer and standard HQAM at the physical layer, was demonstrated in Figures 7 and 8 in the previous subsection. In this subsection, Figures 10 and 11 show the FER curves for the CLD system, with and without the SSD mechanism incorporated at the physical layer. In each case t is equal to 1 and $\alpha = 3$ but the Nakagami m value is 1 and 2 for Figures 10 and 11 respectively. As can be seen in both figures, the incorporation of the HM SSD scheme to the CLD system results in gains throughout the SNR range when compared to the system without the SSD

mechanism implemented. To get a quantified value for the improvement, if a FER target of 10^{-4} for the HP sub-stream is taken, the FER curves in Figure 10 (which is for a Nakagami m=1 channel with HM hierarchy $\alpha = 3$) show that there is a gain of approximately 10dB for the CLD system with SSD HQAM system at the physical layer as compared to the system with the standard HQAM system at the physical layer, and this gain is achieved without the system using any additional transmit power or bandwidth. Another observation that can be made by comparing the graphs in Figures 10 and 11 is that the gain produced by the SSD HQAM system reduces as the channel condition improves. If an FER target of 10^{-4} for the HP sub-stream is once again taken, the graphs for the HP sub-stream in Figure 11 (which is for a Nakagami m=2 channel with HM hierarchy $\alpha = 3$) shows that the gain of the SSD HQAM system over the standard HQAM system is now approximately 3dB. This result is to be expected as the diversity benefits of the SSD scheme reduce as the channel conditions improve, thus conversely, the two layer UEP CLD system with SSD HQAM performs better than the standard HQAM system under deep fading channel conditions.

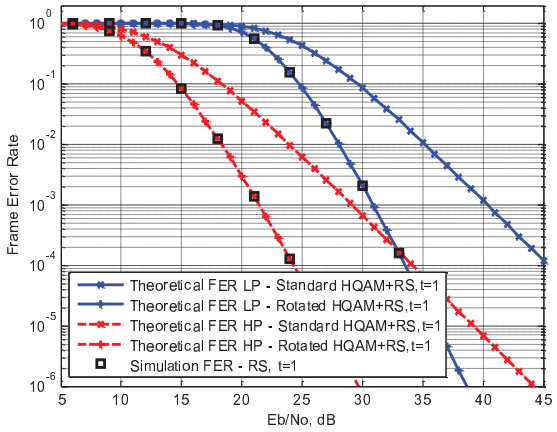

Figure 10: FER of HP and LP streams for two layer UEP CLD in Nakagami-m, m=1, α =3.

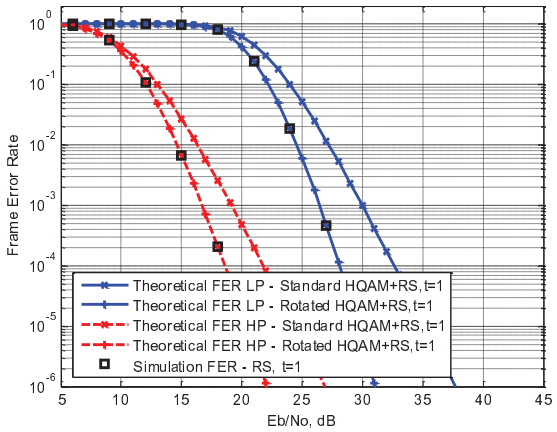

Figure 11: FER of HP and LP streams for two layer UEP CLD in Nakagami-m, m=2, α =3.

6. Conclusion

In this study a framework for a two layer UEP CLD system using RS coding at the application layer coupled with HQAM at the physical layer was presented. It was shown how such a mechanism can provide flexible variable UEP for the transmission of multimedia traffic in a single frame by varying parameters that affect UEP both at the application and physical layers. Furthermore, the inclusion of the SSD HQAM mechanism at the physical layer of the CLD system led to noticeable gains as it was shown that for a FER target of 10^{-4} over a Nakagami m=1 channel, the HM SSD system had a 10dB gain over the standard HM system. The results also showed that these gains were reduced when the channel conditions improved and this leads to the conclusion that the SSD HQAM incorporated CLD system is more effective than the standard HQAM system under deep fading channel conditions. In future work, the proposed system's various adaptable parameters, such as the level of RS error correcting capability; the level of hierarchy using HQAM, will be adapted to channel conditions to design an energy efficient, QoS aware, adaptive cross-layer design system for the transmission of multimedia traffic over fading channels.

Appendix

A. BER expressions for the Decision Boundary Approach

The general BER expressions, $P_b(i_k, M)$, used in (8) and (9) as derived in [16] is shown in (A1).

$$P_b(i_k, M) = P_b(q_k, M) = \frac{1}{\sqrt{M}} \sum_{j=0}^{\left(\frac{\sqrt{M}}{2}\right)-1} I(1, 2j), \quad \text{(A1)}$$

$$\text{For } k > 1: \; P_b(i_k, M) = P_b(q_k, M) \quad \text{(A2)}$$

$$= \frac{1}{\sqrt{M}} \Bigg[\sum_{j=0}^{J(k,M)-1} (-1)^{F[jZ(k,M)]} \times \left[2^{k-1} - 2F\left[j * Z(k,M) + \frac{1}{2} \right] \right] \times I(0, 2j+1) + \sum_{j=0}^{J(k,M)-1} (-1)^{F[jZ(k,M)]} \times F\left[j \times Z(k,M) + \frac{1}{2} \right] \times I(2, 2j-1) + \sum_{j=J(k,M)}^{K(k,M)} (-1)^{F[jZ(k,M)]} \times \left[2^{k-1} - F\left[j \times Z(k,M) + \frac{1}{2} \right] \right] \times I(2, 2j-1) \Bigg]$$

where $F[\cdot]$ is the floor function, $Z(k,M) = \frac{2^{k-1}}{\sqrt{M}}$, $K(k,M) = \sqrt{M}(1 - 2^{-k}) - 1$, $J(k,M) = \sqrt{M}\left(\frac{1}{2} - \frac{1}{2^k}\right)$, $I(a,b) = erfc\left(\sqrt{G(a,b;\alpha,M)\gamma}\right)$ and

$$G(a,b;\alpha,M)=\frac{(a+\alpha b)^2}{\left[2\left[1+\alpha\left[\frac{\sqrt{M}}{2}-1\right]\right]^2+\frac{2}{3}\left[\frac{M}{4}-1\right]\alpha^2\right]} \quad \text{(A3)}$$

The above expressions, which are for additive white Gaussian noise (AWGN) channels, were extended to Nakagami-*m* fading channels in [16]. These expressions (10) and (11) are valid for Nakagami-*m* fading channels with the modification to the $I(a,b)$ function shown in (13), where $\bar{\gamma}$ is the average signal-to-noise ratio (SNR).

$$I(a,b)=\sqrt{\frac{G(a,b;\alpha,M)\bar{\gamma}}{\pi}}*\frac{m^m}{(m+G(a,b;\alpha,M)\bar{\gamma})^{m+\frac{1}{2}}}*\frac{\Gamma\left(m+\frac{1}{2}\right)}{\Gamma(m+1)}*{}_2F_1\left(1,m+\frac{1}{2};m+1;\frac{m}{m+G(a,b;\alpha,M)\bar{\gamma}}\right) \quad \text{(A4)}$$

where ${}_2F_1(.,.;.;)$ is the Gauss hyper-geometric function, m is the Nakagami fading parameter and $\Gamma(\cdot)$ is the gamma function.

B. PEP expressions for the Nearest Neighbourhood Approach

The pairwise error probability (PEP) of perpendicular neighbhouring symbols in adjacent quadrants, $P(X_B \to X_C)$, is given by

$$P(X_B\to X_C)=\frac{1}{4n}\left(\frac{2m}{2m+\bar{\gamma}\ \beta\cos^2\theta}\right)^m\left(\frac{2m}{2m+\bar{\gamma}\ \beta\sin^2\theta}\right)^m+\frac{1}{2n}\sum_{k=1}^{n-1}\left(\frac{mS_k}{mS_k+\bar{\gamma}\beta_1\cos^2\theta}\right)^m\left(\frac{mS_k}{mS_k+\bar{\gamma}\beta_1\sin^2\theta}\right)^m, \quad \text{(B1)}$$

where $\bar{\gamma}$ is the average SNR per hierarchical 16-QAM symbol, θ is the optimum rotation angle from (3), $S_k=2\sin^2(k\pi/2n)$, $\beta_1=\frac{\alpha^2}{\alpha^2+2\alpha+2}$ and n is the number of summations. n greater than 6 will result in an accurate approximation.

The PEP of diagonal neighbouring symbols, $P(X_B \to X_D)$ and $P(X_E \to X_C)$, is given by (B2) and (B3) respectively.

$$P(X_B\to X_D)=\frac{1}{4n}\left(\frac{2m}{2m+\bar{\gamma}\beta_2(\alpha\cos\theta-\sin\theta)^2}\right)^m\left(\frac{2m}{2m+\bar{\gamma}\beta_2(\alpha\sin+\cos\theta)^2}\right)^m+\frac{1}{2n}\sum_{k=1}^{n-1}\left(\frac{mS_k}{mS_k+\bar{\gamma}\beta_2(\alpha\cos\theta-\sin\theta)^2}\right)^m\left(\frac{mS_k}{mS_k+\bar{\gamma}\beta_2(\alpha\sin+\cos\theta)^2}\right)^m, \quad \text{(B2)}$$

$$P(X_E\to X_C)=\frac{1}{4n}\left(\frac{2m}{2m+\bar{\gamma}\ \beta(\alpha\cos\theta+\sin\theta)^2}\right)^m\left(\frac{2m}{2m+\bar{\gamma}\ \beta(\alpha\sin-\cos\theta)^2}\right)^m+\frac{1}{2n}\sum_{k=1}^{n-1}\left(\frac{mS_k}{mS_k+\bar{\gamma}\ \beta(\alpha\cos\theta+\sin\theta)^2}\right)^m\left(\frac{mS_k}{mS_k+\bar{\gamma}\ \beta(\alpha\sin-\cos\theta)^2}\right)^m, \quad \text{(B3)}$$

where $\beta_2=\frac{1}{\alpha^2+2\alpha+2}$.

The PEP of a perpendicular neighbour within the same quadrant, $(X_A \to X_B)$, is given by (B4).

$$P(X_A\to X_B)=\frac{1}{4n}\left(\frac{2m}{2m+\bar{\gamma}\ \beta\cos^2\theta}\right)^m\left(\frac{2m}{2m+\bar{\gamma}\ \beta\sin^2\theta}\right)^m+\frac{1}{2n}\sum_{k=1}^{n-1}\left(\frac{mS_k}{mS_k+\bar{\gamma}\ \beta\cos^2\theta}\right)^m\left(\frac{mS_k}{mS_k+\bar{\gamma}\ \beta\sin^2\theta}\right)^m \quad \text{(B4)}$$

REFERENCES

[1] J. Hossain, P.K. Vitthaladevuni, M.-S. Alouini, V.K. Bhargava, A.J. Goldsmith, "Adaptive hierarchical modulation for simultaneous voice and multiclass data transmission over fading channels," *IEEE Transactions on Vehicular Technology*, vol. 55, issue 4, pp. 1181 – 1194, July, 2006.

[2] H. Mukhtar, M. El-Tarhuni, "An Adaptive Hierarchical QAM Scheme for Enhanced Bandwidth and Power Utilization," *IEEE Transactions on Communications*, vol. 60, issue 8, pp. 2275 – 2284, August, 2012.

[3] S.S. Arslan, P.C. Cosman, L.B. Milstein, "Coded Hierarchical Modulation for Wireless Progressive Image Transmission" *IEEE Transactions on Vehicular Technology,* vol. 60, issue 9, pp. 4299 – 4313, November, 2011.

[4] T. Quazi, H. Xu, F. Takawira, "Quality of Service for Multimedia Traffic using Cross-Layer Design," *IET Communications*, vol. 3, issue 1, pp. 83 – 90, January, 2009.

[5] J. Boutros, E. Viterbo, "Signal Space Diversity: A Power- and Bandwidth-Efficient Diversity Technique for the Rayleigh Fading Channel," *IEEE Transactions on Information Theory*, vol. 44, no. 4, pp. 1453 – 1467, July, 1998.

[6] P. Ma, K.S. Kwak, "Modulation-assisted UEP-LDPC codes in image transmission," *in Proc. IEEE ISCIT*, 2009, pp. 230 – 233.

[7] M. Ghandi, B. Barmada, E. Jones, M.Ghanbari, "Unequally error protected data partitioned video with combined hierarchical modulation and channel coding," *in Proc. IEEE International Conference Acoustics, Speech Signal Process*., 2006, vol. 2, pp. II-529 – II-532.

[8] C. Hellge, T. Schierl, T. Wiegand, "Mobile TV with SVC and hierarchical modulation for DVB-H broadcast services," *in Proc. of the IEEE International Symposium on Broadband Multimedia Systems and Broadcasting,* 2009, pp.1 – 5.

[9] A. Saeed, T. Quazi, H. Xu, "Hierarchical Modulated QAM with Signal Space Diversity and MRC Reception in Nakagami-m fading channels," *IET Communications*, vol. 7, issue 12, pp. 1296 – 1303 , August, 2013.

[10] Z. Hu and H. Liu, "A Low-Complexity LDPC Decoding Algorithm for Hierarchical Broadcasting: Design and Implementation," *IEEE Transactions on Vehicular Technology*, vol. 62, no. 4, pp. 1843 – 1849, May, 2013.

[11] Z. Hu and H. Liu, "Structure-based Decoding for Hierarchically Modulated, LDPC coded Signals," *in Proc. Global Communications Conference 2012*, pp.4036 – 4042.

[12] A. Bouabdallah, D. Pradas, J. Lacan, M. Vazquez Castro, M. Bousquet, "Cross-layer optimization of unequal protected layered video over hierarchical

modulation," *in Proc. IEEE Global Telecomunications Conference,* 2009*,* pp.1 – 6.

[13] L. Vangelista, N. Benvenuto, S. Tomasin, C. Nokes, J. Stott, A. Filippi, M. Vlot, V. Mignone, A. Morello, "Key Technologies for Next-Generation Terrestrial Digital Television Standrad DVB-T2," *IEEE Communications Magazine*, vol. 47, no. 10, pp. 146 – 153, October, 2009.

[14] S. Wang, S. Kwon, and B. K. Yi, "On enhancing hierarchical modulation," *in Proc. of the IEEE International Symposium on Broadband Multimedia Systems and Broadcasting, 2008,* pp.1 – 6.

[15] H. Zhao,X. Zhou,Y. Yang, W. Wang, "Hierarchical Modulation with Vector Rotation for E-MBMS Transmission in LTE Systems, " *Journal of Electrical & Computer Engineering, Hindawi Publishing Corporation*, vol. 2010, pp. 1 – 9, August, 2010.

[16] P.K.Vitthaladevuni, M.S. Alouini, "BER Computation of 4/M-QAM Hierarchial Constellations," *IEEE Transactions on Broadcasting*, vol. 47, issue 3, pp. 228 – 239, September, 2001.

[17] G. Abreu, "Accurate Simulation of Piecewise Continuous Arbitrary Nakagami-m Phasor Processes," *in Proc. IEEE Global Telecommunications Conference*, 2006, pp. 1 – 6.